

Correction of the power law of ac conductivity in ion-conducting materials due to the electrode polarization effect

A. A. Khamzin, I. I. Popov, and R. R. Nigmatullin

Institute of Physics, Kazan (Volga Region) Federal University, Kremlevskaya str.18, Kazan, 420008, Russia

(Received 31 July 2013; revised manuscript received 17 January 2014; published 10 March 2014)

Based on the supposition related to fractal nature of transport processes in ion-conducting materials, an expression for the low-frequency ac conductivity dependence was derived. This expression for the ac conductivity generalizes the power-law dependence and gives a possibility to take into account the influence of the electrode polarization effect. The ac conductivity expression obtained is in excellent agreement with experimental data for a wide frequency range.

DOI: [10.1103/PhysRevE.89.032303](https://doi.org/10.1103/PhysRevE.89.032303)

PACS number(s): 77.22.Gm, 72.80.Ng

I. INTRODUCTION

Ionic conduction in glasses and other disordered solids is a subject of growing interest due to applications in connection with solid-oxide fuel cells, electrochemical sensors, thin-film solid electrolytes in batteries, and supercapacitors, electrochromic windows, oxygen-separation membranes, functional polymers, etc. At the same time, ion conduction in disordered solids remains an area of basic research because a number of fundamental questions are still not settled [1–4].

Usual conductivity spectra consist essentially of two regions, apparently related to two different phenomena. At high frequencies (and low temperatures), the conductive properties are governed by the transport of the charge carriers in the bulk. The underlying mechanism of this contribution represents the (translational) diffusion of ions and is theoretically well understood [4–10]. This part of the spectra can be used to extract important molecular parameters characterizing the hopping mechanism of the charge carriers. At lower frequencies (and higher temperatures), pronounced changes in the complex conductivity function are detected due to presence of solid electrodes, acting on the charge carriers as (nearly) blocking interfaces [11–14]. This part, exhibiting a peculiar dependence on the geometry of the measurement cell (e.g., the cell length) and on the material used for the electrodes, was considered for a long time to be a parasitic effect (“electrode polarization”) and usually cut off from the bulk contribution of the spectra. An alternative approach to describing electrode polarization has been presented by Macdonald [15].

Here, we remark on some important peculiarities of ac conductivity and dielectric permittivity experimental spectra of ion-conducting materials. What one typically observes for ion-conducting materials is a frequency-dependent conductivity and dielectric constant like that shown in Fig. 1. Here, we see a considerable dependence of both quantities on the frequency of the applied electric field. Starting at low frequencies, we find a large increase, which is replaced by the slowdown (accompanied by the decreasing of a slope), with decreasing frequency of the dielectric constant which, in the limit of a dc field, can attain a plateau value. This phenomenon results from the presence of metallic or so-called blocking electrodes, that do not permit transfer of mobile ions into the external measuring circuit. Since the ions are blocked by the metal electrode, there is accumulation or depletion of ions near the electrodes, leading to the formation of space-charge layers.

The voltage drops rapidly in these layers, which implies a huge electrical polarization of the material and a near absence of electric field in the bulk sample at low frequencies. The buildup of electrical polarization and the drop of the electric field in the bulk are reflected in an increase in the ac permittivity and a decrease in the ac conductivity with decreasing frequency. For completely blocking electrodes $\sigma(0) = 0$, that is obvious. Although this “electrode polarization” [16] is a direct result of the ion motion, it is a nonequilibrium, extrinsic feature that depends both upon the nature of the electrode interface and the thickness of the specimen [17]. The most prominent features of electrode polarization are emphasized by arrows in Fig. 1. These effects are coming into play at a certain frequency ω_{on} (“onset of the electrode polarization”), where a steep increase in ϵ' (corresponding to a minimum in σ'') is detected first. At lower frequencies ($\omega \approx \omega_{\text{max}}$, “full development of the electrode polarization”) a slope in ϵ' starts to change (with decreasing from high to low frequencies), corresponding to a peak in σ'' . At the same frequency $\omega \approx \omega_{\text{max}}$ the real part of the conductivity σ' begins to decrease.

As we move to higher frequencies, we observe a short plateau σ_{dc} in the conductivity. In terms of the mean-squared displacement, this so-called dc conductivity represents the long-range diffusion of ions as they hop from site to site through the matrix. In the dielectric constant, we observe a shoulder that suggests an incipient polarization occurring in this same frequency range.

As we move still further up in frequency, we see in Fig. 1 a dramatic increase in $\sigma(\omega)$ and a leveling off in $\epsilon(\omega)$. The leveling off of the dielectric constant occurs because, in addition to the mean-squared displacement of mobile ions, our matrix contains atoms that have become elastically polarized under the influence of the applied field. These atomic and electronic polarizations occur at frequencies well above 1 GHz [18] leaving behind a plateau ϵ_{∞} , atop which the contribution due to nonelastic ion motion rests.

The conductivity increases with increasing frequency in a roughly power-law manner, and in the high-frequency limit the data appear to approach a linear (or superlinear [19]) dependence on frequency. The linear frequency dependence would imply a regime where the dielectric loss is frequency independent, a regime often referred to as the “nearly constant loss” (NCL) regime. The NCL is a feature that is currently much debated ([20–23]) and has created much recent research interest.

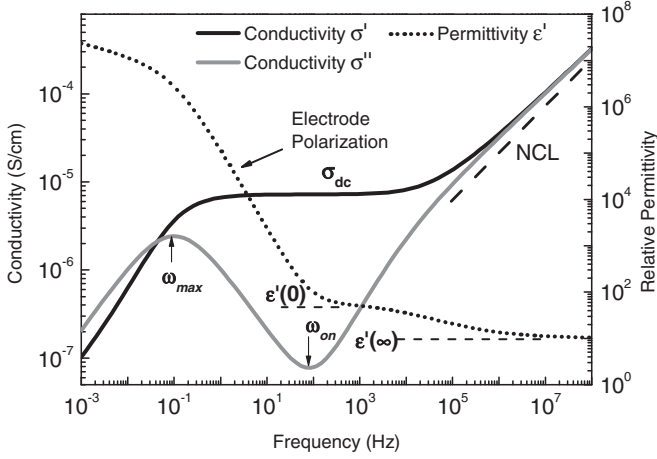


FIG. 1. Schematic representation of how the ac conductivity and dielectric constant typically depend upon frequency for an ionic material. Several of the limiting features are labeled.

Putting all this together, we can approximate the frequency dependence of the ac conductivity, aside from the portion affected by electrode polarization [24], with the following empirical function:

$$\sigma'(\omega) \approx \sigma_0[1 + (\omega/\omega_0)^n] + A\omega. \quad (1)$$

This sort of power-law description of the ac conductivity has been advocated by several authors [25–30]. Values for the exponent n range from 0.5 to 0.7 with a concentration of results near $n = 2/3$ [31,32]. The second term (linear term) in the expression represents the NCL. It should be noted that the separation in Eq. (1) of a fractal power law and a linear term is entirely empirical as experimental data generally exhibit a continuous increase in the logarithmic slope of the ac conductivity with increasing frequency. Nevertheless, some studies [33,20] suggest the NCL regime involves distinctly different kinds of ion movement.

The main purpose of this paper is to suggest an expression for the low-frequency part of the ac conductivity. It generalizes the power-law behavior, when the electrode polarization phenomenon takes place, and confirms the validity of an expression on available experimental data.

II. SELF-CONSISTENT DYNAMIC-RELAXATION MODEL

Let a homogeneous, isotropic dielectric be exposed to the external polarizing electric field $\mathbf{E}(t, \mathbf{r})$, which we consider as a function of time t and the space coordinate \mathbf{r} . By homogeneous and isotropic, we refer to spatial scales larger than the typical scales of the molecular and/or structural disorder. Assuming a linear and spatially local response of the material, the polarization field at time t at point \mathbf{r} can be written as

$$\mathbf{P}(t, \mathbf{r}) = \mathbf{P}(0, \mathbf{r}) + \int_0^t \chi(t - t') \mathbf{E}(t', \mathbf{r}) dt', \quad (2)$$

where $\mathbf{P}(0, \mathbf{r})$ is the initial polarization, $\chi(t)$ is a response or memory function, and $\mathbf{E}(t, \mathbf{r})$ is the electric field. We shall assume that there are no external electric fields acting in the system after time $t = 0$, so that $\mathbf{E}(t, \mathbf{r})$ is essentially the inherent,

self-consistent electric field in the bulk of the dielectric due to the electric charges present.

Let $\rho(t, \mathbf{r})$ be the density of the electric charges at time t at point \mathbf{r} . The function $\rho(t, \mathbf{r})$ is defined as the mean density of the charges in a small volume around \mathbf{r} such that the highly fluctuating molecular densities are averaged out. One assumes that there is a length-scale separation between the microscopic molecular scales and the length scales on which the mean density varies. On length scales comparable to or shorter than the molecular scales, the dynamics of relaxation must be described statistically.

Assume for simplicity that there are no external charges, i.e., the total charge of the medium is zero. The polarization charges are then the only source for the polarization and electric fields, i.e.,

$$\nabla \cdot \mathbf{E}(t, \mathbf{r}) = 4\pi\rho(t, \mathbf{r}) \quad (3)$$

and

$$\nabla \cdot \mathbf{P}(t, \mathbf{r}) = -\rho(t, \mathbf{r}). \quad (4)$$

Hence,

$$\nabla \cdot \mathbf{D}(t, \mathbf{r}) = 0, \quad (5)$$

where $\mathbf{D}(t, \mathbf{r}) = \mathbf{E}(t, \mathbf{r}) + 4\pi\mathbf{P}(t, \mathbf{r})$ defines the electric displacement in the medium. The density of the polarization and/or relaxation currents is defined as the time derivative of the polarization field, i.e., $\mathbf{j}(t, \mathbf{r}) = \partial\mathbf{P}(t, \mathbf{r})/\partial t$. From Eq. (2), we have

$$\mathbf{j}(t, \mathbf{r}) = \int_0^t \sigma(t - t') \mathbf{E}(t', \mathbf{r}) dt', \quad (6)$$

where $\sigma(t) = \partial\chi(t)/\partial t$ is a new memory function. A Fourier transformed $\sigma(t)$ defines the frequency-dependent complex conductivity of the medium, which is related to the susceptibility function via $\sigma(\omega) = i\omega\chi(\omega)$.

The conservation of the electric charge is expressed by the continuity equation $\partial\rho(t, \mathbf{r})/\partial t + \nabla \cdot \mathbf{j}(t, \mathbf{r}) = 0$. Substituting $\mathbf{j}(t, \mathbf{r})$ from Eq. (6), then taking ∇ under the time integration and using Eq. (3), we have

$$\frac{\partial}{\partial t} \rho(t, \mathbf{r}) + 4\pi \int_0^t \sigma(t - t') \rho(t', \mathbf{r}) dt' = 0. \quad (7)$$

By Laplace transforming Eq. (7) we find

$$s\rho(s, \mathbf{r}) - \rho(0, \mathbf{r}) + 4\pi\sigma(s)\rho(s, \mathbf{r}) = 0, \quad (8)$$

where $\rho(0, \mathbf{r})$ is the density of the charges at time $t = 0$, and $\sigma(s)$ is the Laplace transform of $\sigma(t)$. Separating the variables in Eq. (8) we write $\rho(s, \mathbf{r}) = \phi(s)\rho(0, \mathbf{r})$ where $\phi(s)$ defines the Laplace transform of the relaxation function $\phi(t)$. From Eq. (8), it follows that

$$\phi(s) = \frac{1}{s + 4\pi\sigma(s)}, \quad (9)$$

where the initial condition $\phi(0) = 1$ has been applied.

III. CONCEPT OF MEMORY FUNCTION AND ac CONDUCTIVITY

In the frame of the linear-response approximation, the fluctuations of polarization caused by thermal motion are the

same as for the macroscopic dipole relaxation function induced by the electric field [34]. Thus, one can equate approximately the relaxation function and the macroscopic dipole correlation function (DCF) $\psi(t)$ to each other as

$$\phi(t) \cong \psi(t) = \frac{\langle \mathbf{M}(t) \cdot \mathbf{M}(0) \rangle}{\langle \mathbf{M}(0) \cdot \mathbf{M}(0) \rangle}, \quad (10)$$

where $\mathbf{M}(t)$ is the macroscopic fluctuating dipole moment of the sample volume unit, which is equal to the vector sum of all elementary molecular dipoles. The equation that governs by the time evolution of the DCF [or relaxation function $\phi(t)$] is given by the master equation [35]

$$\frac{\partial}{\partial t} \phi(t) = - \int_0^t K_1(t-t') \phi(t') dt', \quad (11)$$

where $K_1(t)$ is the memory kernel of the relaxation process and it contains the full dynamics of the N bodies as it is prescribed by the Liouville equation without any additional assumption. $K_1(t)$ represents the non-Markovian effect (presence of memory) of the correlation function.

Integrating Eq. (11), we present it in the form

$$\phi(t) - 1 = - \int_0^t M_1(t-t') \phi(t') dt', \quad (12)$$

where $M_1(t) = \int_0^t K_1(t-t') dt'$ is the integral memory function (IMF). The usage of the IMF is more preferable because, as a rule, in the construction of the theory of anomalous dielectric relaxation the initial memory function $K_1(t)$ can belong to the space of the generalized functions. The Laplace transform of Eq. (12) leads to the result

$$\phi(s) = \frac{1}{s(1 + M_1(s))}. \quad (13)$$

Comparing the last Eq. (13) with Eq. (9), one can obtain the relationship between conductivity and the Laplace image of the integral memory function

$$\sigma(s) = \frac{sM_1(s)}{4\pi}. \quad (14)$$

It is known [36] that relaxation and transport phenomena in disordered media, being strongly nonequilibrium in their nature, have a hierarchy-subordinated structure. The establishing of the hierarchy subordination leads to the fractal structure of the potential-energy landscape [37]. The fractal character of relaxation and charge carrier transport in the hierarchy-subordinated systems leads to the following property of the memory function $M_1(t)$ [38,39] scale invariance:

$$M_1(\xi t) = \xi^{\alpha-1} M_1(t), \quad (15)$$

where α is a constant, which, as it has been shown in [38,39], determines the fractal dimension of the time-space ensemble characterizing the relaxation process. The power-law function

$$M_1(t) = A_1 \frac{t^{\alpha-1}}{\Gamma(\alpha)} \quad (16)$$

(A_1 is a constant) is the partial solution of the functional (15). The substitution of the Laplace image of the memory function $M_1(t)$ (16) in Eq. (14) leads to the power-law behavior of

conductivity

$$\sigma(s) = \frac{A_1}{4\pi} s^{1-\alpha}, \quad (17)$$

which coincides (at $s = i\omega$) with the power-law behavior term that enters into Eq. (1) for ac conductivity. In the frame of the memory function formalism, there is a real possibility to justify another term figuring in Eq. (1). As it has been mentioned in the Introduction to this paper, there are the contributions of the NCL and dc regimes, which are governed by different types of ionic motion.

Some types (for certainty considered as independent) of ionic motions in the frame of the memory function formalism one can associate with additive contributions to the total memory function [40,41]: $M_1(t) = \sum_{k=1}^n M_{1k}(t)$. We choose these additional terms to the memory function in the form of power-law functions with different exponents: $M_{1k}(t) = A_k t^{\alpha_k-1}$. Because the contribution of the term to the NCL regime in the frequency domain is approximately linear, then this type of ionic motion corresponds to the memory function with $\alpha = 0$:

$$M_{\text{INCL}}(t) = A_{\text{NCL}} t^{-1}. \quad (18)$$

But, for this function the corresponding Laplace transform is absent. For overcoming of this difficulty we realize the integration for the expression $M_{\text{INCL}}(t)$ and obtain the function

$$N_{\text{INCL}}(t) = A_{\text{NCL}} \ln(t/t_N), \quad (19)$$

where t_N defines a relatively short temporal scale of the NCL regime of ion motion. The relationship between the formal Laplace transform of the function $M_{\text{INCL}}(t)$ and Laplace image of the function $N_{\text{INCL}}(t)$ has the form

$$M_{\text{INCL}}(s) = s N_{\text{INCL}}(s). \quad (20)$$

Taking into account the known expression for the Laplace image of the function $\ln t$ and Eq. (14), one can find the following expression for the NCL contribution to ac conductivity:

$$\sigma_{\text{NCL}}(s) = \frac{sM_{\text{INCL}}(s)}{4\pi} = \frac{s^2 N_{\text{INCL}}(s)}{4\pi} = -\frac{A_{\text{NCL}} s}{4\pi} \ln(s/\omega_N), \quad (21)$$

where $\omega_N = 1.78107/t_N$. Putting here $s = i\omega$ and extracting the real and imaginary parts, one can obtain the expressions $\sigma'_{\text{NCL}}(\omega)$, $\sigma''_{\text{NCL}}(\omega)$ for the NCL contribution:

$$\sigma'_{\text{NCL}}(\omega) = \frac{\pi}{2} \sigma_N \frac{\omega}{\omega_N}, \quad (22)$$

$$\sigma''_{\text{NCL}}(\omega) = \sigma_N \frac{\omega}{\omega_N} \ln\left(\frac{\omega_N}{\omega}\right), \quad (23)$$

where the following notation is used: $\sigma_N = A_{\text{NCL}} \omega_N / 4\pi$.

By analogy, one can evaluate the contribution of the dc conductivity, connecting it with an additive contribution to the memory function $M_1(t)$ with the power-law exponent $\alpha = 1$: $M_{\text{1dc}}(t) = A_{\text{dc}} = 4\pi\sigma_0$. Finally, we obtain

$$\sigma_{\text{dc}}(s) = \frac{sM_{\text{1dc}}(s)}{4\pi} = \sigma_0. \quad (24)$$

As it follows from Eq. (14), the Laplace images of conductivity and the function $N_1(t)$ are connected with each

other by means of the relationship $\sigma(s) = s^2 N_1(s)/4\pi$. If we take into account the result of [42], where the frequency dependence of conductivity is determined by the Fourier transform of the mean-squared displacement

$$\sigma(\omega) = -\omega^2 \frac{Nq^2}{6T} \lim_{\delta \rightarrow 0} \int_0^\infty \langle r^2(t) \rangle \exp(-i\omega t - \delta t) dt, \quad (25)$$

then we find $N_1(t) \propto \langle r^2(t) \rangle$. So, based on these two relationships, one can reproduce easily the well-known expressions for the mean-squared displacement [43]

$$\langle r^2(t) \rangle_{dc} \propto t, \quad \langle r^2(t) \rangle_{ac} \propto t^\alpha, \quad \langle r^2(t) \rangle_{NCL} \propto \ln t. \quad (26)$$

IV. CORRECTION OF THE POWER LAW OF ac CONDUCTIVITY IN PRESENCE OF “ELECTRODE POLARIZATION” EFFECT

However, the contribution to the ac conductivity of a type (17) does *not* enable us to describe completely the whole low-frequency range of the total conductivity spectrum, when the electrode polarization effect takes place. So, there is a necessity for obtaining a general expression for the ac conductivity, which gives a possibility to describe the behavior of this function for the whole low-frequency range. For the solution of this problem, it is necessary to develop a theoretical approach for a small-time domain that will correspond to the high-frequency range extension. In the frame of the Mori formalism [35], there is a possibility of such kind; it is associated with the necessity of evolution consideration of the memory function $K_1(t)$. In turn, for consideration of its evolution, it is necessary to bond this memory function with the memory function of the second order $K_2(t)$ by means of the following equation [35]:

$$\frac{\partial}{\partial t} K_1(t) = - \int_0^t K_2(t-t') K_1(t') dt'. \quad (27)$$

In Eq. (27), the kernel $K_2(t)$ accounts for the time lag effects produced by the internal mechanism, which ultimately represents the ensemble average of the fluctuation torques dynamics acting on a representative dipole of the system.

Introducing the integral second-order memory function $M_2(t) = \int_0^t K_2(t-t') dt'$ and performing the double integration of Eq. (27) initially in the limits from t up to ∞ [taking into account the conditions $K_1(t \rightarrow \infty) = 0$ and $M_2(t \rightarrow \infty) = 0$] and then integrating in the limits $(0, t)$, one can transform finally Eq. (27) to the following integral equation:

$$M_1(t) + \int_0^t M_2(t-t') M_1(t') dt' = b, \quad (28)$$

where b determines the constant of integration. It is found from the condition

$$b = \int_0^t M_2(t-t') M_1(t') dt' |_{t \rightarrow \infty}. \quad (29)$$

The Laplace transform of Eq. (28) leads to the result

$$M_1(s) = \frac{b}{s(1 + M_2(s))}. \quad (30)$$

Let us *suppose* that the function $M_2(t)$ satisfies to the scaling invariance condition (15) that will correspond to the

fractal character of the current-current correlation function evolution. As a result, we obtain the power-law behavior for the function $M_2(t)$: $M_2(t) = A_2 t^{\alpha-1} / \Gamma(\alpha)$, where A_2 is a constant. Using the expression for the Laplace image of the obtained function $M_2(t)$: $M_2(s) = A_2 s^{-\alpha}$ one can find easily the following expression for the Laplace image of the function $M_1(t)$:

$$M_1(s) = \frac{b}{s(1 + A_2 s^{-\alpha})}. \quad (31)$$

Choosing the constant A_2 in the form $A_2 = \tau_J^{-\alpha}$ and coming back to the time domain in Eq. (31), one obtains

$$M_1(t) = b E_\alpha[-(t/\tau_J)^\alpha], \quad (32)$$

where $E_\alpha[z]$ is the Mittag-Leffler function. At small times ($t < \tau_J$), expression (32) for $M_1(t)$ is approximated by the stretched exponent as $M_1(t) \approx b \exp[-(t/\tau_J)^\alpha / \Gamma(1 + \alpha)]$, where the temporal parameter τ_J determines the characteristic relaxation time of the current-current correlation function.

The derived expression for the function $M_1(t)$ [Eq. (32)] with Eqs. (14) and (31) determines the following frequency behavior for ac conductivity:

$$\sigma(s = i\omega) \equiv \sigma_{\text{frac}}(\omega) = \frac{b}{4\pi(1 + (i\omega\tau_J)^{-\alpha})}. \quad (33)$$

This equation generalizes the conventional ac conductivity expression and it was determined as the “universal” Jonsher’s correction [45]. It takes into account the influence of the electrode polarization effect on the whole spectrum of the complex conductivity.

V. VERIFICATION OF THE GENERALIZED FREQUENCY-DEPENDENT CONDUCTIVITY ON EXPERIMENTAL DATA

Taking into account the contribution of the conductivity at constant electrical field $\sigma_0 = \sigma(0)$ and high-frequency contribution of dielectric relaxation, one can write the following expression for the total conductivity:

$$\sigma_{\text{tot}}(\omega) = \sigma_0 + \frac{\sigma_{dc} - \sigma_0}{1 + (i\omega/\omega_J)^{-\alpha}} + i\omega\varepsilon_0[\varepsilon_{\text{relax}}(\omega) - \varepsilon_\infty], \quad (34)$$

where we introduce the notations $b = 4\pi(\sigma_{dc} - \sigma_0)$, $\omega_J = 1/\tau_J$, and exclude the current of the bounded charges $\varepsilon_0(\varepsilon_\infty - 1)i\omega$ [6]; here, $\varepsilon_0 = 8.85 \times 10^{-12} \text{F/m}$ is the dielectric permittivity of a vacuum. We should stress here that in the presence of the electrode polarizations effect $\sigma_0 = \sigma(0)$ does not coincide with the value σ_{dc} which is shown in Fig. 1. Expression $\varepsilon_{\text{relax}}(\omega)$ determines the contribution of the dielectric relaxation part. From Eq. (34), one can obtain the following form for the frequency behavior of dielectric permittivity [$\varepsilon(\omega) - \varepsilon_\infty = \sigma_{\text{tot}}(\omega)/(i\omega\varepsilon_0)$]:

$$\varepsilon(\omega) = \frac{\sigma_0}{i\omega\varepsilon_0} + \frac{\sigma_{dc} - \sigma_0}{i\omega\varepsilon_0(1 + (i\omega/\omega_J)^{-\alpha})} + \varepsilon_{\text{relax}}(\omega). \quad (35)$$

In absence of the dipole relaxation or in supposition that the relaxation loss peak is situated in the high-frequency range, we can define that $\varepsilon_{\text{relax}}(\omega) \approx \varepsilon_s$. In the result of this

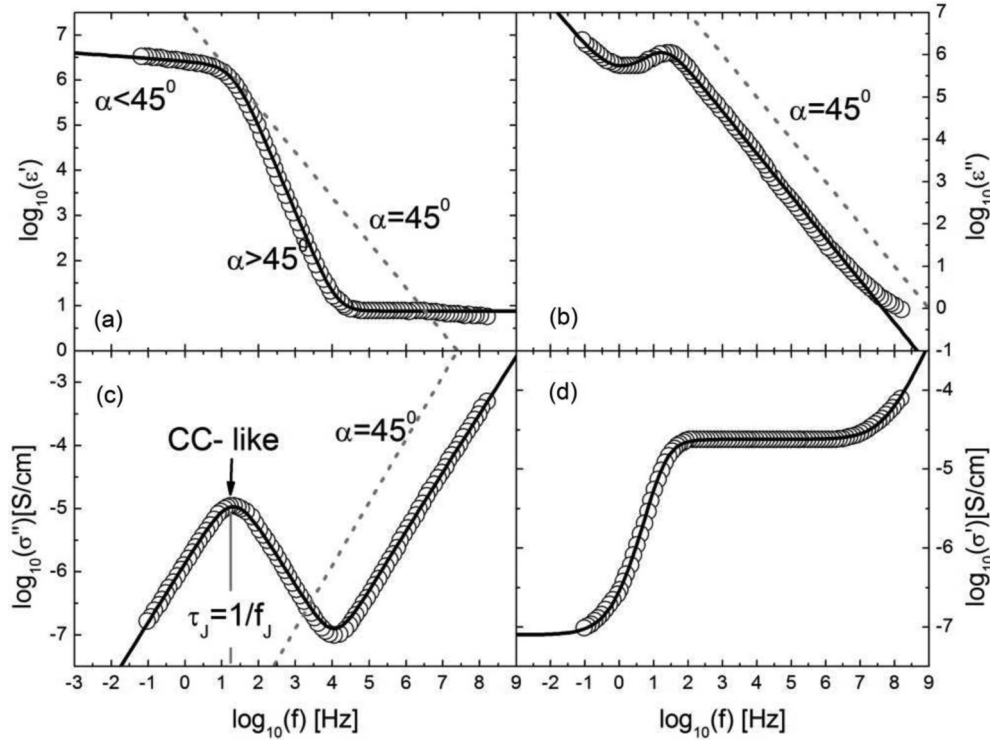


FIG. 2. Complex dielectric permittivity and conductivity of 1-hexyl-3-methylimidazolium hexafluorophosphate (HMIM-PF6) versus frequency at 264 K [44]. Open circles are experimental points, the solid black line represents the fitting curve that corresponds to functions (35) and (36).

approximation, Eq. (34) is simplified and accepts the form

$$\sigma(\omega) = \sigma_{dc} - \frac{\sigma_{dc} - \sigma_0}{1 + (i\omega/\omega_J)^\alpha} + i\omega\varepsilon_0\Delta\varepsilon, \quad (36)$$

where $\Delta\varepsilon = \varepsilon_s - \varepsilon_\infty$.

The imaginary part of the found expression (36) for the ac conductivity is determined by the following formulas:

$$\begin{aligned} \sigma''(\omega) &= \text{Im}[\sigma(\omega)] \\ &= \varepsilon_0\omega_J\Delta\varepsilon e^x + \frac{(\sigma_{dc} - \sigma_0)\sin(\pi\alpha/2)}{2(\cosh(\alpha x) + \cos(\pi\alpha/2))}, \\ x &= \ln(\omega\tau_J) \end{aligned} \quad (37)$$

and it is changed nonmonotonically with changing of the current frequency (or the value x). This behavior is typical for the electrode polarization effect (see Fig. 1). One can find from the given expression (37) the values of frequencies that correspond to the positions of extreme points:

$$\begin{aligned} \frac{d\sigma''(x)}{dx} &= \varepsilon_0\omega_J\Delta\varepsilon e^x \\ &- \frac{\alpha(\sigma_{dc} - \sigma_0)\sin(\pi\alpha/2)\sinh(\alpha x)}{2(\cosh(\alpha x) + \cos(\pi\alpha/2))^2} = 0 \Rightarrow \\ x_{\max} &= \ln(\omega_{\max}/\omega_J) \approx \frac{2(1 + \cos(\pi\alpha/2))^2}{\alpha^2\sin(\pi\alpha/2)} \frac{\omega_J\varepsilon_0\Delta\varepsilon}{\sigma_{dc} - \sigma_0}, \\ x_{\text{on}} &= \ln(\omega_{\text{on}}/\omega_J) \approx \frac{1}{1 + \alpha} \ln\left[\frac{\sigma_0 - \sigma_{dc}}{\omega_J\varepsilon_0\Delta\varepsilon} \alpha \sin\left(\frac{\pi\alpha}{2}\right)\right]. \end{aligned} \quad (38)$$

The found values of frequencies ω_{on} , ω_{\max} determine the characteristic frequencies that correspond to the “onset of the electrode polarization” and “full development of the electrode polarization” accordingly (see Fig. 1).

Now, we are ready to verify the main peculiarities of frequency behavior of Eqs. (35) and (36) on available data. As an example, we use experimental data of 1-hexyl-3-methylimidazolium hexafluorophosphate (HMIM-PF6) at 264 K that were taken from [44]:

(1) As one can see from Eq. (37), the imaginary part of conductivity (without relaxation term) has Cole-Cole form with a “tail” shifted to the high-frequency range. In log-log scale, this “tail” is transformed to a straight line with tangent of slope equal to 45° . It is shown on Fig. 2(c).

(2) The real part of conductivity has also Cole-Cole form but it is inverted in the frequency range, i.e., the step-function increases with the growth of a frequency. It is shown on Fig. 2(d).

(3) For the real part of dielectric permittivity at relatively frequencies $\omega_J \ll \omega$, we have from Eq. (35)

$$\ln\{\text{Re}[\varepsilon(\omega)]\} \approx -(\alpha + 1)\ln(\omega) + \text{const}. \quad (39)$$

Because of $0 < \alpha < 1$, the curve (39) has a slope *exceeding or even* 45° . At low frequencies ($\omega \ll \omega_J$) the curve has the form

$$\ln\{\text{Re}[\varepsilon(\omega)]\} \approx (\alpha - 1)\ln(\omega) + \text{const}, \quad (40)$$

with the slope that should be less than 45° . The behavior of the imaginary part of (35) strongly depends on the value of σ_0 . If σ_0

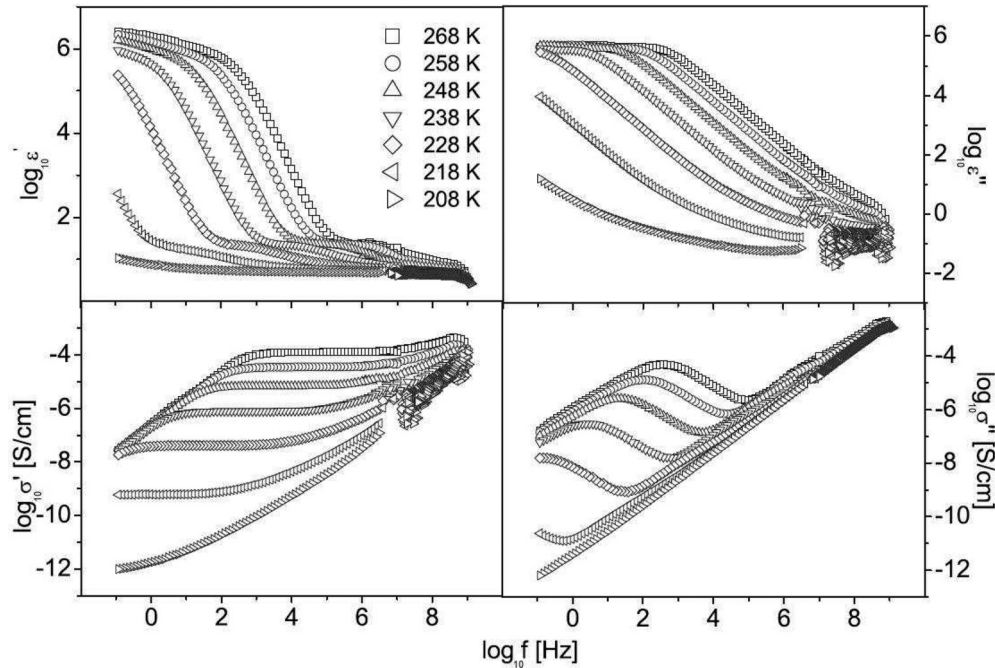


FIG. 3. Complex dielectric function and complex conductivity of dimethylimidazolium dimethylphosphate (MMIM-Me2PO4) as a function of frequency at different temperatures, as indicated [47].

accepts the large value in comparison with the remaining terms in (35), then in log-log scale we obtain a line with the slope equal to 45°. If the value σ_0 is becoming less in comparison with the remaining terms, then the function (35) in this case at $\omega \gg \omega_J$ has the expression

$$\ln\{\text{Im}[\varepsilon(\omega)]\} \approx -\ln(\omega) + \text{const}, \quad (41)$$

with the slope equal to 45°. For the case when $\omega \ll \omega_J$ we obtain another approximate expression

$$\ln\{\text{Im}[\varepsilon(\omega)]\} \approx -(1 - \alpha)\ln(\omega) + \text{const}, \quad (42)$$

from which it follows that the curve has the slope that is less than or equal to 45°. Thus, in log-log scale, the imaginary and real parts of the ac conductivity at low frequencies have an inflection point at certain frequency. It is shown on Figs. 2(a) and 2(b).

From analysis of these plots it follows that there is a possibility of evaluation of the characteristic relaxation-time value of the current-current correlation function τ_J ; (a) based on the positions of the frequencies f_{on} , f_{max} or (b) using the specific points that correspond to the slope changing in the frequency dependence of the logarithm of the real part of dielectric permittivity.

The appearance of the ac conductivity correction (33) in the frequency domain is caused by the electrode polarization phenomenon and is related to existence of the, so-called, “fractal” current [45], which, in turn, is caused by the self-similar (fractal) structure of the electrode surfaces. This idea was proposed in [46]. Therefore, we want to represent another experimental data set, where the electrode polarization phenomena take place in order to add some additional proofs for validity of Eq. (33). On Figs. 3 and 4, experimental data of dimethylimidazolium dimethylphosphate and polyethylene oxide methacrylate are presented (they are

taken from papers [47,48], correspondingly). From these figures it follows that these dielectric permittivity curves have the bend in the region $10^0 - 10^1$ Hz. The imaginary part of conductivity has the Cole-Cole type form with a “tail” at high frequencies also. As for the curve tangent loss ($\tan\delta$) presented in the small frame of Fig. 4 [as one can verify easily from (35)], it should have bell-like behavior (see [45,49] for detail).

Then, we consider experimental data where the so-called NCL regime is expressed clearly. On Fig. 5, we demonstrate the frequency dependencies of the functions ε'' and σ'' at different temperatures of polymer electrolyte consisting of polyethylene oxide (PEO) and LiCF_3SO_3 with molar ratio of ether oxygens (EO) to lithium ions $\text{EO/Li} = 30$,

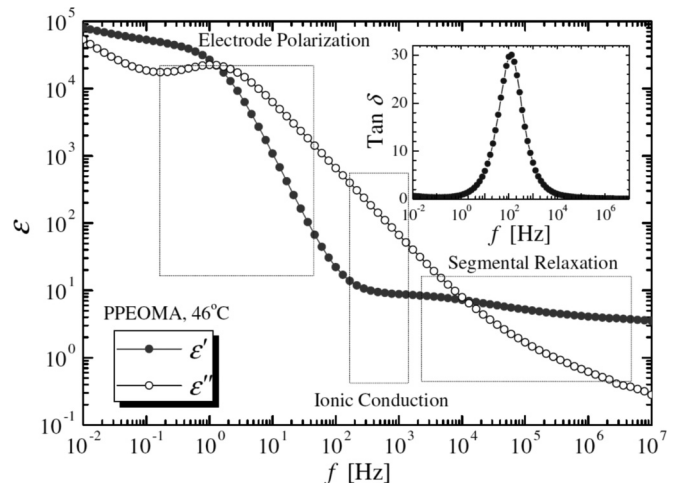


FIG. 4. Dielectric spectrum for polyethylene oxide methacrylate (PPEOMA) at 46°C. In the small frame, $\tan\delta$ loss is shown [48].

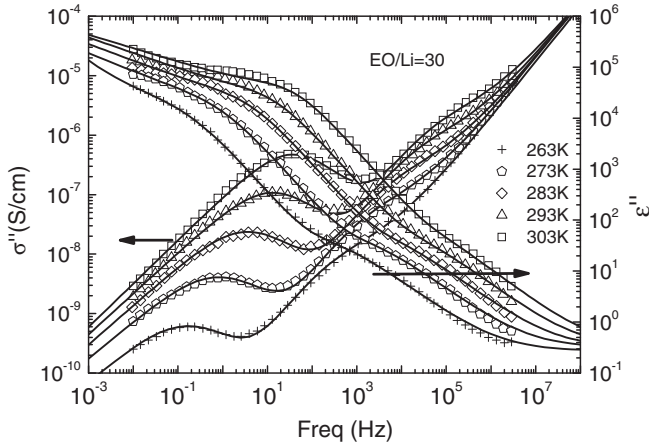


FIG. 5. Frequency dependence of ϵ'' and σ'' at different temperatures of polymer electrolyte consisting of polyethylene oxide (PEO) and LiCF_3SO_3 with $\text{EO/Li} = 30$ [50].

taken from paper [50]. As one can notice from Fig. 5, two phenomena (electrode polarization and NCL regime) take place. Taking into account the mathematical expression for the NCL (21), the total expressions for the frequency dependencies of dielectric permittivity and ac conductivity accept the form

$$\epsilon(\omega) = \frac{\sigma_0}{i\omega\epsilon_0} + \frac{\sigma_{\text{dc}} - \sigma_0}{i\omega\epsilon_0(1 + (i\omega/\omega_J)^{-\alpha})} - \frac{\sigma_N}{\epsilon_0\omega_N} \ln\left(\frac{i\omega}{\omega_N}\right) + \epsilon_s, \quad (43)$$

$$\sigma(\omega) = \sigma_{\text{dc}} - \frac{\sigma_{\text{dc}} - \sigma_0}{1 + (i\omega/\omega_J)^\alpha} - \sigma_N \frac{i\omega}{\omega_N} \ln\left(\frac{i\omega}{\omega_N}\right) + i\omega\epsilon_0\Delta\epsilon. \quad (44)$$

Expressions for extreme frequencies ω_{on} , ω_{max} with additional contribution from the NCL regime can be written as

$$x_{\text{max}} = \ln(\omega_{\text{max}}/\omega_J) \approx \frac{2(1 + \cos(\pi\alpha/2))^2}{\alpha^2 \sin(\pi\alpha/2)} \times \left(\frac{\omega_J \epsilon_0 \Delta\epsilon}{\sigma_{\text{dc}} - \sigma_0} + \frac{\sigma_N}{(\sigma_{\text{dc}} - \sigma_0)} \frac{\omega_J}{\omega_N} \ln\left[\frac{\omega_N}{e\omega_J}\right] \right),$$

$$x_{\text{on}} = \ln(\omega_{\text{on}}/\omega_J) \approx \frac{\epsilon_0 \Delta\epsilon}{\sigma_N} \omega_N. \quad (45)$$

On Fig. 5, we demonstrate the results of the fitting (solid lines) of the experimental data points realized with the help of the curves (43) and (44). Notice the excellent agreement between the suggested theoretical curves and independently measured experimental data.

VI. CONCLUSION

In conclusion of this paper, we want to stress the following fact. The excellent agreement of the modified ac conductivity expression tested on the available measured data demonstrates the consistency of the theoretical approach associated with consideration of the transport phenomena in ion-conducting materials, where the electrode polarization phenomenon takes place. The basic idea of this theoretical approach is related to the self-similar evolution of current-current correlation function, which determines and mainly explains the anomalies of the transport properties observed.

The modified correction to the ac conductivity (33), as it was demonstrated in this paper, describes perfectly the frequency behavior of the ac conductivity and permittivity for a relatively low range of frequencies. For this range, the electrode polarization effect takes place. In order to increase the frequency range and understand the behavior of the ac conductivity in ion-conducting materials, it is necessary to take into account other types of ionic motions, in particular the NCL regime. Different types of ion motion in the frame of the proposed formalism can be associated with an additive contribution to the memory function. Allowances for the contribution of the NCL regime lead us to expression (44) for the ac conductivity. It allows us to describe the experimental data for more wide frequency range and confirms the experimentally established fact that at frequencies above the “dc regime,” the derivative $d\ln(\sigma')/d\ln(f)$ has a tendency to increase with increasing of the current frequency continuously. The further increasing of a frequency window for description of experimental data for $\sigma'(\omega)$ is possible and can be associated with more detailed evaluation of the dipole relaxation term. Really, if one chooses (for certainty) the Cole-Cole expression for relaxation part of the dielectric permittivity

$$\epsilon_{\text{relax}}(\omega) = \epsilon_\infty + \frac{\Delta\epsilon}{1 + (i\omega/\omega_R)^\nu} \approx_{\omega \ll \omega_R} \epsilon_s - \Delta\epsilon \left(\frac{i\omega}{\omega_R}\right)^\nu, \quad (46)$$

where the stretching power-law exponent lies in the interval $0 < \nu < 1$, and ω_R determines the characteristic frequency of dipole relaxation then [as it follows from (34)] and taking into account the NCL contribution term expression for $\sigma'(\omega)$ accepts the form

$$\sigma'(\omega) = \sigma_{\text{dc}} - (\sigma_{\text{dc}} - \sigma_0) \frac{1 + (\omega/\omega_J)^\alpha \cos(\pi\alpha/2)}{1 + 2(\omega/\omega_J)^\alpha \cos(\pi\alpha/2) + (\omega/\omega_J)^{2\alpha}} + \frac{\pi}{2} \sigma_N \frac{\omega}{\omega_N} + \omega_R \epsilon_0 \Delta\epsilon \sin\left(\frac{\pi\nu}{2}\right) \left(\frac{\omega}{\omega_R}\right)^{1+\nu}. \quad (47)$$

Equation (47) allows us to describe experimental data for wide range of frequencies including the region above the dc conductivity. In log-log scale, the slope of the frequency dependence of the function $\sigma'(\omega)$ with the growth of frequency increases continuously from the value of α to the unit value and then gradually to the value $1 + \nu$.

[1] M. D. Ingram, *Phys. Chem. Glasses* **28**, 215 (1987).

[2] C. A. Angell, *Chem. Rev.* **90**, 523 (1990).

[3] J. Maier, *Prog. Solid State Chem.* **23**, 171 (1995).

[4] J. C. Dyre, P. Maass, B. Roling, and D. L. Sidebottom, *Rep. Prog. Phys.* **72**, 046501 (2009).

[5] J. C. Dyre and T. B. Schroder, *Phys. Rev. B* **54**, 14884 (1996).

- [6] J. C. Dyre and T. B. Schroder, *Rev. Mod. Phys.* **72**, 873 (2000).
- [7] T. B. Schroder and J. C. Dyre, *Phys. Rev. Lett.* **84**, 310 (2000).
- [8] K. Funke, R. D. Banhatti, S. Bruckner, C. Cramer, C. Krieger, A. Mandanici, C. Martiny, and I. Ross, *Phys. Chem. Chem. Phys.* **4**, 3155 (2002).
- [9] K. Funke and R. D. Banhatti, *Solid State Ionics* **169**, 1 (2004).
- [10] K. Funke and R. D. Banhatti, *Solid State Ionics* **177**, 1551 (2006).
- [11] P. Kohn, K. Schröter, and T. Thurn-Albrecht, *Phys. Rev. Lett.* **99**, 086104 (2007).
- [12] R. J. Klein, S. Zhang, S. Dou, B. H. Jones, R. H. Colby, and J. Runt, *J. Chem. Phys.* **124**, 144903 (2006).
- [13] S. Uemura, *J. Polym. Sci., Polym. Phys. Ed.* **12**, 1177 (1974).
- [14] *Impedance Spectroscopy: Theory, Experiment, and Applications*, edited by E. Barsoukov and J. R. Macdonald (Wiley, New York, 2005).
- [15] J. R. Macdonald, *J. Phys.: Condens. Matter* **17**, 4369 (2005).
- [16] P. B. Macedo, C. T. Moynihan, and R. Bose, *Phys. Chem. Glasses* **13**, 171 (1972).
- [17] J. M. Hyde, M. Tomozawa, and M. Yoshiyagawa, *Phys. Chem. Glasses* **28**, 174 (1987).
- [18] A. K. Jonscher, *Dielectric Relaxation in Solids* (Chelsea Dielectrics, London 1983).
- [19] C. Cramer, K. Funke, T. Saatkamp, D. Wilmer, and M. D. Ingram, *Z. Naturforsch* **50**, 613 (1995).
- [20] K. L. Ngai, *J. Chem. Phys.* **110**, 10576 (1999).
- [21] A. Rivera, C. Leon, C. P. E. Varsamis, G. D. Chryssikos, K. L. Ngai, C. M. Roland, and L. J. Buckley, *Phys. Rev. Lett.* **88**, 125902 (2002).
- [22] S. Murugavel and B. Roling, *J. Non-Cryst. Solids* **330**, 122 (2003).
- [23] D. L. Sidebottom, *Phys. Rev. B* **71**, 134206 (2005).
- [24] J. R. Macdonald, *J. Electroanal. Chem.* **378**, 17 (1994).
- [25] A. K. Jonscher, *Nature (London)* **267**, 673 (1977).
- [26] D. P. Almond and A. R. West, *Solid State Ionics* **9–10**, 277 (1983).
- [27] D. P. Almond and A. R. West, *Solid State Ionics* **11**, 57 (1983).
- [28] D. P. Almond, G. K. Duncan, and A. R. West, *Solid State Ionics* **8**, 159 (1983).
- [29] S. R. Elliott, *Solid State Ionics* **70–71**, 27 (1994).
- [30] A. S. Nowick, A. V. Vaysleyb, and W. Liu, *Solid State Ionics* **105**, 121 (1998).
- [31] D. L. Sidebottom, P. F. Green, and R. K. Brow, *J. Non-Cryst. Solids* **183**, 151 (1995).
- [32] J. R. Macdonald, *Phys. Rev. B* **71**, 184307 (2005).
- [33] D. L. Sidebottom, P. F. Green, and R. K. Brow, *Phys. Rev. Lett.* **74**, 5068 (1995).
- [34] G. William, *J. Chem. Rev.* **72**, 55 (1972).
- [35] H. Mori, *Prog. Theor. Phys.* **33**, 423 (1965); **34**, 399 (1965).
- [36] K. Binder and A. P. Joung, *Rev. Mod. Phys.* **58**, 801 (1986).
- [37] A. I. Olemskoi and V. F. Klepikov, *Phys. Rep.* **338**, 571 (2000).
- [38] A. A. Khamzin, R. R. Nigmatullin, and I. I. Popov, *Theor. Math. Phys.* **173**, 1604 (2012).
- [39] A. A. Khamzin, R. R. Nigmatullin, and I. I. Popov, *Phys. A (Amsterdam)* **392**, 136 (2013).
- [40] I. I. Popov, R. R. Nigmatullin, and A. A. Khamzin, *J. Non-Cryst. Solids* **358**, 1516 (2012).
- [41] A. A. Khamzin, R. R. Nigmatullin, I. I. Popov, and B. A. Murzaliev, *Fract. Calc. Appl. Anal.* **16**, 158 (2013).
- [42] B. Roling, C. Martiny, and S. Bruckner, *Phys. Rev. B* **63**, 214203 (2001).
- [43] D. L. Sidebottom, *Rev. Mod. Phys.* **81**, 999 (2009).
- [44] A. Serghei, M. Tress, J. R. Sangoro, and F. Kremer, *Phys. Rev. B* **80**, 184301 (2009).
- [45] I. I. Popov, R. R. Nigmatullin, E. Yu. Koroleva, and A. A. Nabereznov, *J. Non-Cryst. Solids* **358**, 1 (2012).
- [46] S. H. Liu, *Phys. Rev. Lett.* **55**, 529 (1985).
- [47] J. R. Sangoro, A. Serghei, S. Naumov, P. Galvosas, J. Kärger, C. Wespe, F. Bordusa, and F. Kremer, *Phys. Rev. E* **77**, 051202 (2008).
- [48] Y. Wang, A. L. Agapov, F. Fan, K. Hong, X. Yu, J. Mays, and A. P. Sokolov, *Phys. Rev. Lett.* **108**, 088303 (2012).
- [49] I. I. Popov, R. R. Nigmatullin, A. A. Khamzin, and I. V. Lounev, *J. Appl. Phys.* **112**, 094107 (2012).
- [50] N. K. Karan, D. K. Pradhan, R. Thomas, B. Natesan, and R. S. Katiyar, *Solid State Ionics* **179**, 689 (2008).